2021 43rd Annual International Conference of the
IEEE Engineering in Medicine & Biology Society (EMBC)
Oct 31 - Nov 4, 2021. Virtual Conference

Correction of Electrode ID Configuration based on Distribution of Surface EMG Features

Takashi Isezaki, Ryosuke Aoki and Yukio Koike

Abstract— **Surface EMG (sEMG) signals are useful for estimating the motion or exercise of users. Wireless-type sensor electrodes, which are placed on multiple parts of the body and send the measured signals to a server, have recently become commercially available. With many estimation algorithms, the relationships between the sensor IDs and the body parts they are placed on (ID configuration) are expected to be fixed between the calibration and estimation phases. If the ID configuration is changed after the calibration phase, the estimation accuracy tends to dramatically decrease. Since it is inconvenient for users to check the ID configuration every time, we developed a method to correct the electrode ID configuration on the basis of the distribution of sEMG features. Using open data, we investigated the feasibility of our method by shuffling the order of sEMG signals. The results showed that the method was able to correct the ID configuration and restore the estimation accuracy to close to that of the calibration.**

I. INTRODUCTION

Surface EMG (sEMG), which occurs when the muscles shrink, is a physiological signal measured from the surface of the skin. Past studies have proposed methods that estimate the motion or exercise of users on the basis of the sEMG signals [1], [2]. Obtaining users' motion is useful for several applications such as lifelogging and robot control. If the electrodes are placed the same as they are in the calibration, high estimation accuracy is expected.

A Garment-type physiological signal measurement system, which does not require users to put electrodes, is one of the promising approaches[3]. However, there is noise in the measured signals during motions because electrodes are not fixed on the skins. Therefore, a wireless-type sensor system such as the Trigno Avanti sensor (Delsys Inc.), which is attachable on the skins, is another promising approach. For daily measurement, users need to attach the sensor electrodes at the start of use and then take them off at the end. In order to ensure high accuracy, the electrodes need to be placed at the same location for both the calibration and the estimation. However, sometimes subtle displacement occurs after the calibration phase even if the same electrode is placed on the same muscle, which leads to a decrease in estimation accuracy. Several studies have examined how to avoid such displacement [4], [5], and recently it has become more feasible.

However, there is another placement drawback when it comes to the wireless-type sensor electrodes. Each sensor electrode in the system is assigned an ID that enables it to communicate with the server. While it is assumed that each electrode at the same location has the same ID between the calibration and estimation phases, past research has shown that displacement tends to occur on the surface of a body part. This is problematic because, in many estimation algorithms, the relationship between the sensor ID and the body part it is placed on (ID configuration) is expected to be fixed between the calibration and estimation phases. To obtain high estimation accuracy, in addition to the placement, the ID configuration of each electrode must be matched between the two phases. However, it is inconvenient for the user to check the IDs of each electrode one by one and make adjustments. Re-calibration at the start of use is also considered bothersome for users. These system-derived drawbacks may discourage the use of such wireless-type sensor electrodes in daily measurement.

The ideal scenario is that users will simply pick up the sensor electrodes without having to check the IDs and then place them onto the desired muscle or body part. The purpose of this study is to correct the ID configuration automatically so that users do not have to check or adjust it. During the correction of the ID configuration and estimation of users' motion, the true label of users' motion is not available, so the requirement is to correct the ID configuration by using the sEMG features obtained from randomly shuffled ID configurations without labels of motion. Our contributions are (1) proposing a novel way to correct the ID configuration of the electrodes on the basis of the distribution of sEMG features, (2) investigating the feasibility of our method by using the Ninapro database that includes sEMG data from multiple hand motions of healthy subjects [6], [7].

II. METHOD

Fig. 1 shows the overview of the proposed method. The goal is to calculate a transformation matrix $\hat{\boldsymbol{M}}$ to correct the ID configuration. In the case shown in Fig. 1, the order of measured signals, (e^1, e^2, e^3, e^4), is based on the ID configuration. However, the placement of the electrodes (ID configuration) is different between the calibration and estimation phases. For example, e^1 (red circle) in the estimation phase is placed at the e^4 (black circle) location in the calibration phase. The signals of e^1 between the two phases are different because the location is different. In terms of correction, the signal of e^3 (blue circle) in the estimation phase needs to be used as the signal of e^1 in the calibration phase of the ID configuration. Therefore, we use a transformation matrix $\hat{\boldsymbol{M}}$ for correcting the ID configuration,

Takashi Isezaki, Ryosuke Aoki and Yukio Koike are with NTT Human Informatics Laboratories, Nippon Telegraph and Telephone Corporation, Japan. takashi.isezaki.xd@hco.ntt.co.jp

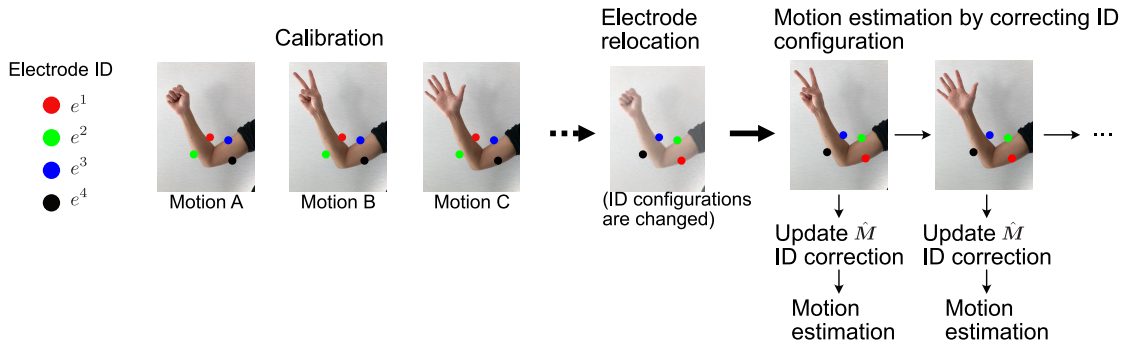

Fig. 1. Overview of proposed method. The circles show the placement of electrodes, and different colors (red, blue, green, and black) indicate each ID. In the calibration phase, the sEMG signals of motions to be estimated are measured and an estimation model is constructed at the ID configuration. The ID configurations are assumed to be different between the calibration and estimation phases due to relocation of the electrodes. The proposed method calculates a transformation matrix to correct the ID configuration in the estimation phase so that it matches that of the calibration phase.

as

$$\begin{pmatrix} e^1_{cal} \\ e^2_{cal} \\ e^3_{cal} \\ e^4_{cal} \end{pmatrix} = \hat{\boldsymbol{M}} \begin{pmatrix} e^1_{est} \\ e^2_{est} \\ e^3_{est} \\ e^4_{est} \end{pmatrix} \tag{1}$$

$$\hat{\boldsymbol{M}} = \begin{pmatrix} 0 & 0 & 1 & 0 \\ 0 & 0 & 0 & 1 \\ 0 & 1 & 0 & 0 \\ 1 & 0 & 0 & 0 \end{pmatrix} \tag{2}$$

where e^1_{cal}, e^2_{cal}, e^3_{cal}, and e^4_{cal} are the signals measured in the calibration, and e^1_{est}, e^2_{est}, e^3_{est}, and e^4_{est} are the signals measured in the estimation. The proposed method calculates the transformation matrix $\hat{\boldsymbol{M}}$ on the basis of the input sEMG signals whose motion labels are unknown.

To correct the ID configuration, our method performs signal processing consisting of the following five steps for each sEMG measurement.

- Measurement of sEMG
- Calculation of features
- Calculation of temporary transformation matrix $\boldsymbol{M}$ for input sEMG feature $\boldsymbol{x}$
- Update of transformation matrix $\hat{\boldsymbol{M}}$
- Estimation of label of motion

Measurement of sEMG: sEMG signals are measured through the wireless-type n_{ch} electrodes. The electrodes are placed at the same position as the calibration but the ID configuration is randomized. A 10–500 Hz bandpass filter is applied to all measured signals. As root mean square (RMS) is a major component for estimating motion, RMS values are calculated from each measured sEMG signal.

Calculation of features: Statistical features are a major component of EMG-based motion estimation [1]. In this paper, we calculate six types of statistical features—$median, average, std, max, min, and ptp$—from each RMS of the electrode signal. $median$ is the median value, $average$ feature is the averaged value, std is the value of standard deviation, max is the maximum value, min is the minimum value, and ptp is the range of values (maximum - minimum) in the extracted signals. Several calculation window sizes have been investigated for estimating motions [8], [9], and in this study, the calculation window with a duration experimentally set to 2.0 [s] is applied to each signal overlapping with 1.0 [s] based on the previous research [8]. Each feature is calculated from each extracted signal based on the extraction window.

An sEMG feature $\boldsymbol{X} = [\boldsymbol{x}^f]$ $f \in [median, average, std, amax, amin, ptp]$ is calculated on the basis of the input sEMG. An element of $\boldsymbol{X}$ whose feature is f is expressed as

$$\boldsymbol{x}^f = [x^f_q] \qquad q = (1, \cdots, n_{ch}) \tag{3}$$

where x^f_q is feature f of the signal measured from the electrode whose ID is q.

Calculation of transformation matrix $\boldsymbol{M}$ for input sEMG feature $\boldsymbol{X}$: Algorithm 1 expresses the calculation of $\boldsymbol{M}$ on the basis of the input sEMG features. $\boldsymbol{M}$ is a plausible matrix to transform the order of the electrode IDs of sEMG features $\boldsymbol{X}$. The dimension of $\boldsymbol{M}$ depends on the number of measured sEMG channels n_{ch}, and is $(n_{ch} \times n_{ch})$. In every row and column of $\boldsymbol{M}$, one element holds 1 and the others hold 0. In the initialization, all elements of $\boldsymbol{M}$ are set to 0.

In the calculation phase, the distribution of sEMG feature $\boldsymbol{X}$ is compared to that of training datasets assuming each label in the training data as the label of the input sEMG feature $\boldsymbol{X}$. In the training dataset, pairs of sEMG feature $\boldsymbol{d}$ and label l are stored. There are multiple sEMG features whose labels are the same in the training dataset. $\boldsymbol{d}^f_{l,i}$ is the feature f of the i-th data in the dataset whose label is l in the training data, and holds n_{ch} feature values, the same as $\boldsymbol{x}^f$. Function $\arg\min_{\boldsymbol{m}} |\boldsymbol{d}^f_{l,i} - \boldsymbol{m}\boldsymbol{x}^f|$ returns the transformation matrix $\boldsymbol{m}^f_{l,i}$, which makes the distribution of the vector $\boldsymbol{x}^f$ close to $\boldsymbol{d}^f_{l,i}$ based on descending sort. Function $g(\boldsymbol{d}^f_{l,i}, \boldsymbol{m}^f_{l,i}\boldsymbol{x}^f)$ returns the mean absolute error between $\boldsymbol{d}^f_{l,i}$ and $\boldsymbol{m}^f_{l,i}\boldsymbol{x}^f$. c is the data index of the training dataset whose label is l, and is the index that minimizes the mean absolute error of $\boldsymbol{d}^f_{l,i}$ and $\boldsymbol{m}^f_{l,i}\boldsymbol{x}^f$ in terms of

Algorithm 1 Calculate Transformation Matrix $\boldsymbol{M}$

Input: sEMG features $\boldsymbol{X}$
Output: Transformation Matrix $\boldsymbol{M}$

Initialization $\boldsymbol{M}$:
for Each element M in $\boldsymbol{M}$ **do**
$M \leftarrow 0$
end for

Calculation $\boldsymbol{M}$:
for $l = 1, \cdots, L$ **do**
for $f \in feature\_types$ **do**
for $i = 1, \cdots, n_l$ **do**
$\boldsymbol{m}^f_{l,i} = \arg\min_{\boldsymbol{m}} |\boldsymbol{d}^f_{l,i} - \boldsymbol{m}\boldsymbol{x}^f|$
end for
$c = \arg\min_{i \in (1,\cdots,n_l)} g(\boldsymbol{d}^f_{l,i}, \boldsymbol{m}^f_{l,i}\boldsymbol{x}^f)$
$\hat{l} = h(\boldsymbol{m}^f_{l,c}\boldsymbol{x}))$
if $\hat{l} = l$ **then**
$\boldsymbol{M} = \boldsymbol{M} + \boldsymbol{m}^f_{l,c}$
end if
end for
end for

Nomarlization $\boldsymbol{M}$:
for $j = 1, \cdots, n_{ch}$ **do**
for $k = 1, \cdots, n_{ch}$ **do**
$M[j][k] \leftarrow M[j][k]/sum(M[j])$
end for
end for

feature f. The transformation matrix $\boldsymbol{m}^f_{l,c}$ is the candidate for the transformation matrix $\boldsymbol{M}$. $h(\boldsymbol{m}^f_{l,c}\boldsymbol{x})$ returns the estimated label $\hat{l}$. If the estimated label $\hat{l}$ is the same as l, the candidate transformation matrix $\boldsymbol{m}^f_{l,c}$ is considered as a valid transform matrix and is added to transformation matrix $\boldsymbol{M}$. This calculation is conducted for each label l and each feature $f \in [median, average, std, amax, amin, ptp]$.

At the end of calculation, transformation matrix $\boldsymbol{M}$ is normalized so that the elements in each row fit from 0 to 1 through the normalization calculation. $M[j][k]$ is the element of the j-th row of the k-th column in $\boldsymbol{M}$.

Update of transformation matrix $\hat{\boldsymbol{M}}$: After the calculation of transformation matrix $\boldsymbol{M}$, the transformation matrix $\hat{\boldsymbol{M}}$ that was held in the system is updated as

$$\hat{\boldsymbol{M}} = \hat{\boldsymbol{M}} + \alpha \boldsymbol{M} \tag{4}$$

where $\hat{\boldsymbol{M}}$ is the transformation matrix over time-series sEMG features, and α is the mixing ratio of $\boldsymbol{M}$, which is calculated from the most recent input sEMG features. In order to converge the transformation matrix $\hat{\boldsymbol{M}}$, α is also decayed in accordance with the input of data. The initial α and decay ratio are tentatively set to 0.2 and 0.98, respectively.

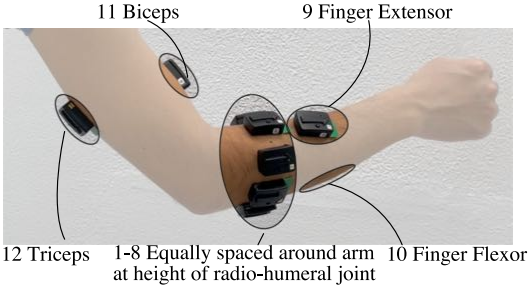

Fig. 2. Placement of the 12 electrodes on the arm. The electrode on the finger flexor is occluded by the arm and therefore not visible in this image. Details are written in [6].

To make a transformation matrix for correcting the ID configuration, all elements must be discrete values. Moreover, one element in each row and column must be set to 1, and the other elements must be set to 0. However, the elements in the updated transformation matrix $\hat{\boldsymbol{M}}$ hold continuous values. Therefore, exclusive normalization is conducted. Our idea here is to extract an element whose value is maximum in $\hat{\boldsymbol{M}}$ and set it to 1, and set the other elements in the same row and column to 0. By repeating this calculation, the transformation matrix $\hat{\boldsymbol{M}}$ is determined.

Estimation of label of motion: The support vector machine (SVM) is a major algorithm for estimating motions based on sEMG features [8], [10], [11]. We construct an SVM-based estimation model using a training dataset and then use the model as $h(\boldsymbol{m}^f_{l,c}\boldsymbol{x})$ in Algorithm 1. The motion label is then estimated by calculating $h(\hat{\boldsymbol{M}}\boldsymbol{x})$.

III. Experiment

We investigated the proposed method using Ninapro database2 (an open database), which includes 12 channels of sEMG data of multiple hand motions from multiple subjects [6]. Fig. 2 shows the electrode placement. This database was constructed through experiments based on approval by the Ethics Commission of the Canton Valais (Switzerland). In this experiment, we used the data of 40 subjects and 17 kinds of motions (Exercise A). Each motion was repeated six times. The first three samples of each motion were used as the training dataset, and the following three were used as the test dataset.

The SVM-based motion label estimation model was calculated using the training dataset. As for the test data, the order of signals was shuffled so that the ID configuration was different from the training dataset, and the order of the labels was also shuffled to consider the effect of task order. The features were calculated as described in Sec. II from the training and test datasets. The test dataset was used for evaluating the estimation accuracy.

The objective of the proposed method is to restore the estimation accuracy to that of the calibration. A restoration ratio $r_{corrected}$ was used for the validation of the proposed method using the accuracy through the ID configuration correction, and the ratio $r_{baseline}$ based on the accuracy without ID configuration correction was used as a baseline.

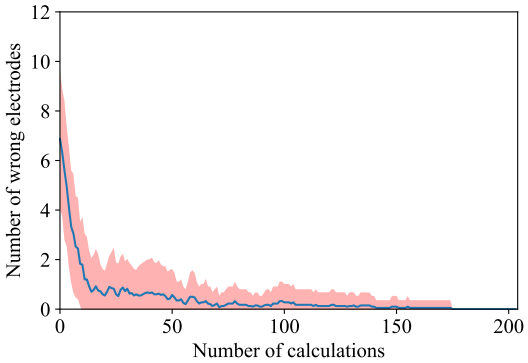

Fig. 3. An example of time-series number of wrong electrodes.

Restoration ratio $r_{corrected}$ and $r_{baseline}$ were formulated by

$$r_{corrected} = \frac{1}{40}\sum_{s=1}^{40}\frac{acc^s_{corrected}}{acc^s_{original}} \quad (5)$$

$$r_{baseline} = \frac{1}{40}\sum_{s=1}^{40}\frac{acc^s_{baseline}}{acc^s_{original}} \quad (6)$$

where $acc^s_{corrected}$ and $acc^s_{baseline}$ are the accuracy with and without the proposed method of s-th subject, respectively. $acc^s_{original}$ is the accuracy under the same ID configuration as the calibration of s-th subject. Restoration ratio $r_{corrected}$ and $r_{baseline}$ were calculated ten times by shuffling the order of the signals.

IV. RESULTS

TABLE I

AVERAGE RATIO AGAINST CALIBRATION PLACEMENT.

Without correction	With correction(proposed)
0.196 (std:0.0096)	0.966 (std:0.0032)

Table. I shows the restoration ratio of the proposed method and baseline. A Wilcoxon rank sum test revealed a significant difference between the ratios (p-value: 0.00195). Fig. 3 shows an example of temporal characteristics of the number of wrong electrodes. This number in each calculation was calculated for each subject. The blue line in the figure indicates the average number of wrong electrodes among subjects. The red shaded area indicates the standard deviation of each calculation.

V. DISCUSSION

From our comparison of the restoration ratios (Table. I), we can see that the proposed method corrected the ID configuration accurately and restored the estimation accuracy to that under the ID configuration in the calibration. The average restoration ratio (0.966) of the proposed method should be feasible for daily measurement if the accuracy of the calibration is sufficient. As shown in Fig. 3, the wrong number of electrodes was close to 0. As for the time-series characteristic, it did not decrease linearly but tended to decrease rapidly in the first 10 to 20 calculations. This characteristic is expected to lead to a rapid improvement in estimation accuracy immediately after the start of use.

In this experiment, the labels of the motion were the same between the training and test datasets. This means that the proposed method works if the labels in the training dataset cover the motions in practical use. However, we did not investigate cases where the motion labels were included in the test dataset but not the training dataset, nor when the motion labels were included in the training dataset but not the test dataset. This is a limitation of the current study and should be investigated in future work. In this paper, we investigated the proposed method by using a database that includes the sEMG data of upper limbs. The applicability to other body parts should also be investigated. There is also another limitation in that we only investigated the proposed method on the basis of statistical features. As frequency features also contribute to the motion estimation, the applicability to frequency features should be evaluated in further experiments.

REFERENCES

[1] J. Kim, S. Mastnik, and E. André, "Emg-based hand gesture recognition for realtime biosignal interfacing," in *Proceedings of the 13th international conference on Intelligent user interfaces*, 2008, pp. 30–39.

[2] Y. Gu, D. Yang, Q. Huang, W. Yang, and H. Liu, "Robust emg pattern recognition in the presence of confounding factors: Features, classifiers and adaptive learning," *Expert Systems with Applications*, vol. 96, pp. 208–217, 2018, ISSN: 0957-4174.

[3] T. Isezaki, H. Kadone, A. Niijima, R. Aoki, T. Watanabe, T. Kimura, and K. Suzuki, "Sock-type wearable sensor for estimating lower leg muscle activity using distal emg signals," *Sensors*, vol. 19, no. 8, 2019, ISSN: 1424-8220. [Online]. Available: https://www.mdpi.com/1424-8220/19/8/1954.

[4] A. Stango, F. Negro, and D. Farina, "Spatial correlation of high density emg signals provides features robust to electrode number and shift in pattern recognition for myocontrol," *IEEE Transactions on Neural Systems and Rehabilitation Engineering*, vol. 23, no. 2, pp. 189–198, 2015. DOI: 10.1109/TNSRE.2014.2366752.

[5] L. Hargrove, K. Englehart, and B. Hudgins, "A training strategy to reduce classification degradation due to electrode displacements in pattern recognition based myoelectric control," *Biomedical Signal Processing and Control*, vol. 3, no. 2, pp. 175–180, 2008, Surface Electromyography, ISSN: 1746-8094.

[6] M. Atzori, A. Gijsberts, C. Castellini, B. Caputo, A.-G. M. Hager, S. Elsig, G. Giatsidis, F. Bassetto, and H. Müller, "Electromyography data for non-invasive naturally-controlled robotic hand prostheses," *Scientific Data*, vol. 1, no. 1, p. 140 053, 2014, ISSN: 2052-4463.

[7] M. Atzori and H. Müller, "The ninapro database: A resource for semg naturally controlled robotic hand prosthetics," in *2015 37th Annual International Conference of the IEEE Engineering in Medicine and Biology Society (EMBC)*, 2015, pp. 7151–7154. DOI: 10.1109/EMBC.2015.7320041.

[8] M. Kunapipat, P. Phukpattaranont, P. Neranon, and K. Thongpull, "Sensor-assisted emg data recording system," in *2018 15th International Conference on Electrical Engineering/Electronics, Computer, Telecommunications and Information Technology (ECTI-CON)*, IEEE, 2018, pp. 772–775.

[9] Z. Zhang, K. Yang, J. Qian, and L. Zhang, "Real-time surface emg pattern recognition for hand gestures based on an artificial neural network," *Sensors*, vol. 19, no. 14, p. 3170, 2019.

[10] S. Benatti, B. Milosevic, F. Casamassima, P. Schönle, P. Bunjaku, S. Fateh, Q. Huang, and L. Benini, "Emg-based hand gesture recognition with flexible analog front end," in *2014 IEEE Biomedical Circuits and Systems Conference (BioCAS) Proceedings*, IEEE, 2014, pp. 57–60.

[11] Z. Xiao, C. Menon, and Z. Khokhar, "Surface emg pattern recognition for real-time control of a wrist exoskeleton," 2010.